

Hybrid Semiconducting Polymer Nanoparticles as Polarization-Sensitive Fluorescent Probes

Maxwell B. Zeigler, Wei Sun, Yu Rong, and Daniel T. Chiu*

Department of Chemistry, University of Washington, Seattle, Washington 98195-1700, United States

S Supporting Information

ABSTRACT: Much work has been done on collapsed chains of conjugated semiconducting polymers and their applications as fluorescent probes or sensors. On surfaces spin-coated with semiconducting polymers, excitation energy transfer along the polymer backbone can be used to quickly and efficiently funnel energy to chromophores with localized energy minima. If each chromophore is immobilized within its matrix, this can result in a large fluorescence anisotropy. Through nanoprecipitation of a matrix polymer blended at low mass ratios with short-chain, hydrophobic, fluorescent semiconducting polymers, we took advantage of this large fluorescence anisotropy to make polarization-sensitive nanoparticles (NPs). These NPs are small (~7 nm in diameter), exhibit a high quantum yield of 0.75, and are easily functionalized to bind to protein targets. Excitation of the NPs with polarized light on a wide-field fluorescence microscope enabled monitoring of both protein location and changes in protein orientation.

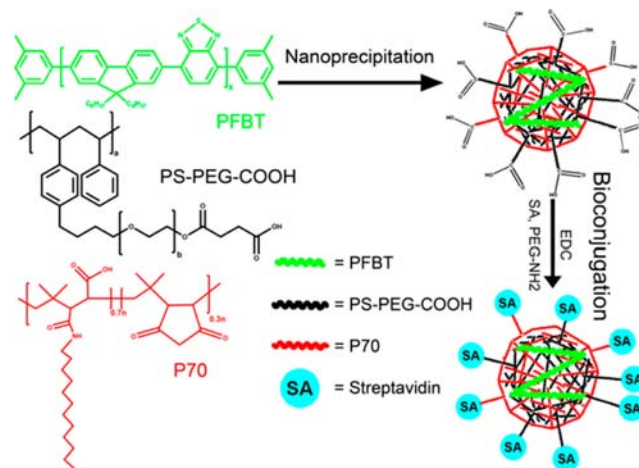
Semiconducting polymer nanoparticles (NPs) offer many advantages as fluorescent tags.¹ They are bright,² emitting enough photons to be tracked with nanometer accuracy.³ They can be made easily from a wide range of fluorescent polymers by nanoprecipitation,^{4,5} allowing the absorption and emission spectra to be tailored to the specific application.⁶ The small size and close packing of the polymers allow for efficient energy transfer to doped dyes.⁷ The NPs can possess flexible surface chemistry and are easily functionalized with antibodies or other proteins^{7–10} to bind a wide array of targets with a high degree of specificity. They can also be incorporated with other NPs, such as quantum dots (QDs) or gold or iron NPs.¹¹ A variety of polymers used to form semiconducting NPs have been shown to be biocompatible.¹²

Electronically excited conjugated polymers in NPs undergo excitation energy transfer (EET) along the polymer chain¹³ and transfer absorbed energy to segments where light emission takes place.¹⁴ This occurs by transfer of energy from higher-energy local regions on a semiconducting polymer chain to lower-energy regions where emission is preferred.^{15–17} By blending fluorescent conjugated polymers at low mass ratios with matrix polymers, we synthesized fluorescent NPs with immobilized chain segments with high fluorescence polarization anisotropy. Monitoring the changes in polarized fluorescence intensity allows changes in NP position to be inferred. When polymer NPs are attached to a protein of interest, observing the changes in the

intensity of polarized light enables changes in protein orientation as well as spatial information to be obtained simultaneously. We demonstrate the practical application of our bright, polarization-sensitive protein probes by monitoring the rotation of microtubules as they precess across a kinesin-coated surface.

Preparation of polymer NPs. Scheme 1 shows the strategy used to prepare the polarization-sensitive fluorescent NPs. Nano-

Scheme 1. Preparation of Polymer NPs by Nanoprecipitation and Subsequent Bioconjugation^a



^aA solution of PFBT, the amphiphilic polymer PS-PEG-COOH, and the matrix polymer P70 in THF is quickly injected into water under high sonication power to precipitate NPs. The hydrophobic fluorescent PFBT is trapped within the cores of the NPs. After removal of THF by heating and bubbling the solution with N₂, the NPs are bioconjugated to SA and PEG. Although both P70 and PS-PEG-COOH are amphiphilic and should fulfill the same role within the NPs, it was found empirically that adding both polymers afforded the smallest NPs with the greatest sensitivity to excitation polarization and the most polarized emission.

precipitation of the hydrophobic fluorescent polymer poly[(9,9-dioctylfluorenyl-2,7-diyl)-*alt-co*-(1,4-benzo-(2,1',3)-thiadiazole)] (PFBT) along with the matrix polymers P70 (see Scheme 1 for chemical formula) and carboxyl-functionalized polystyrene-*g*-poly(ethylene oxide) (PS-PEG-COOH) formed small fluorescent NPs with a mean diameter of 7.5 nm and a peak width of 1.5 nm. The absorption/emission spectra of the NPs are shown in Figure 1A. The NPs were functionalized with streptavidin

Received: May 16, 2013

Published: July 29, 2013

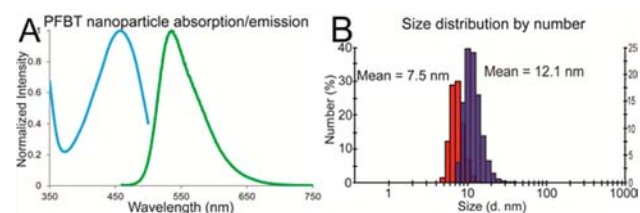


Figure 1. (A) Absorption and emission spectra of polymer NPs. (B) Number-averaged NP hydrodynamic diameter (red) before and (purple) after functionalization.

(SA) to facilitate binding to biomolecules. The NPs had a relatively low ζ potential of -28 mV in 20 mM HEPES buffer at pH 7.2 (Figure S1 in the Supporting Information). To prevent aggregation and nonspecific adsorption, they were also functionalized with PEG. Dynamic light scattering showed an increase in average hydrodynamic diameter (R_h) from 7.46 to 12.07 nm (peak fwhm = 1.46 and 3.72 nm, respectively) due to bioconjugation (Figure 1B). The resulting functionalized NPs were found to be quite monodisperse, and their size measurement remained stable for months at 4 °C. The small size of the polymer NPs generated by this method is valuable because it allows the NPs to bind to proteins with minimal influence on the protein activity and increases the labeling efficiency relative to larger fluorescent tags (e.g., beads) as a result of improved mass transfer properties.

The mass of a single polymer NP was estimated to be 200 kDa by differential centrifugation with a 1.5 M sucrose pillow, corresponding to an ~ 8 nm diameter polymer NP with a density of ~ 1.1 g/cm³. With a 1–5% mass ratio of 10 kDa fluorescent polymer, each polymer NP contained ~ 1 PFBT chain. This low mass ratio of fluorescent polymer differentiates these NPs from previous work with Pdots, which generally contain at least 50% and often up to 100% polymer by mass.^{1,6} Poisson statistics indicates that some of the NPs contained no fluorescent polymer, but the presence of the nonfluorescing NPs did not seem to affect the other NPs. Although the lower mass ratio of PFBT may decrease the brightness of the polymer NPs in comparison to Pdots, it has other photophysical benefits. We previously discussed the formation of PFBT Pdots, which contained 80% PFBT and exhibited a quantum yield of 0.3.^{1,2} In contrast, these polymer NPs were found to have a quantum yield of 0.75 (Figure S2), which is even greater than the quantum yield of PFBT in THF solution. The high quantum yield was likely caused by the minimization of quenching by interchain aggregation^{15,16} as well as reduced collisional quenching of the photoluminescence by the solvent¹⁷ because the amphiphilic polymers protect the hydrophobic fluorescent polymer from the aqueous environment. The polymer NPs were quite photostable, and their brightness was nearly identical to that of QDs upon excitation at 488 nm (Figures S3 and S4).

Polarization sensitivity. The emission intensity of the polymer NPs depended strongly on the polarization of the light used for excitation. To demonstrate this, we used an optical setup with carefully positioned polarizers and $\lambda/2$ waveplates to generate linearly polarized excitation with an excitation polarization intensity ratio (I_{\parallel}/I_{\perp}) of 100:1 measured after the objective. This polarized light selectively excites chromophores whose absorption dipoles are aligned with the light; when the chromophores are confined to a specific orientation, the emitted light can be polarized.¹⁸ The emitted light was separated into its orthogonally polarized components as reported previously,¹⁹ and the

components were imaged onto an EMCCD camera. Information on the orientation changes of the polymer NPs could be deduced from the changes in the intensities of the polarized components of the emitted light.

The dependence of the fluorescence intensity on the light polarization was monitored by two methods (Figure 2A).

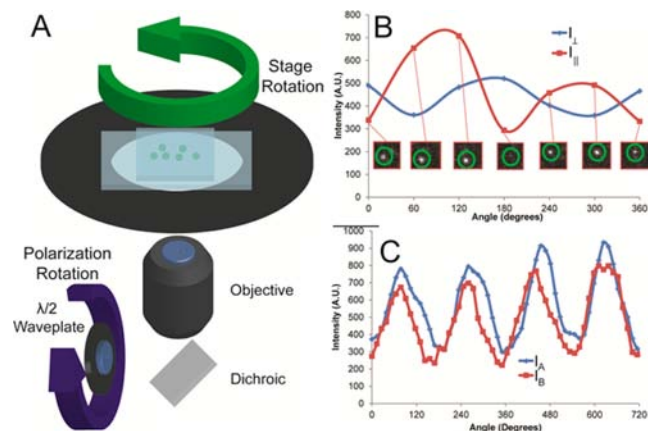


Figure 2. (A) Schematic showing the microscope stage and polymer NPs in a channel. The stage was rotated at constant polarization, or the polarization excitation was changed by rotation of the $\lambda/2$ plate with the stage fixed. (B) Emitted light from a single polymer NP separated into two channels with orthogonal polarizations, plotted as a function of rotation angle of the stage at constant excitation polarization. The emission shows a strong dependence upon the orientation of the single polymer NP. Inset are images of a single NP upon stage rotation captured by the I_{\parallel} channel. (C) Emitted light from a single polymer NP as the excitation polarization was varied by rotating the $\lambda/2$ plate. The correlated intensity change in the orthogonally polarized emission channels, labeled I_A and I_B , was what would be expected from a single emitting chromophore.

Polymer NPs were adsorbed on the surface of a cleaned, APTES-coated glass channel, which was then filled with Milli-Q water. In the first method, the excitation polarization remained fixed while the polymer NP sample was rotated manually using a rotation stage. The resulting anticorrelated intensity maxima and minima for the orthogonally polarized emitted light are shown in Figure 2B. The emission intensities measured in the I_{\parallel} and I_{\perp} channels as the stage was rotated were not always anticorrelated; their relationship depended on the orientation at which the polymer NP was adsorbed to the coverslip. The orientations of the NP emission dipoles were random, so the curves for I_{\parallel} and I_{\perp} could be correlated (as in Figure 2C), anticorrelated, or somewhere in between, depending on the orientation of the dipole moment with respect to the coverslip. Although the maxima and minima were present, practical issues resulting from manual repositioning of the rotation stage somewhat distorted the curves. In the second method, a $\lambda/2$ waveplate placed in the excitation path was rotated while the sample remained stationary. Figure 2C shows I_A and I_B emitted from a single polymer NP, which resembled what would be observed for a single, stationary fluorophore.

The mean molecular mass of the PFBT polymer used in the NPs was 10 kDa, corresponding to an average of 20 chromophores per polymer chain. Each fluorescent monomer was ~ 1.5 nm in length, so in order for the polymer chain to fit inside a 7 nm diameter NP, there must have been kinks in the chain. These kinks created sections of polymer chain that were local energy minima and were preferential for photon emission.²⁰ Intrachain EET to these regions allowed these polymer chains to

behave similarly to single fluorophores.²¹ Also, the polarization can spontaneously increase when excitation energy is trapped at such local minima,²² favoring polarized light emission from the polymer NPs.

Figure 3A depicts EET within a polymer NP. PFBT absorbs photons aligned with its absorption dipole, and the absorbed

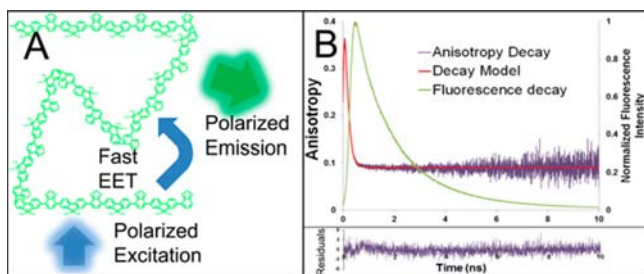


Figure 3. (A) EET within a polymer NP. The fluorescent PFBT is held within the hydrophobic core of the NP. Upon excitation with polarized light, intramolecular exciton transfer quickly directs the energy to chromophores within the polymer chain where fluorescent emission is favored. (B) Overlay of the time-resolved fluorescence anisotropy decay (purple) with the fluorescence lifetime decay (green) of PFBT NPs, showing that emission depolarization occurs more quickly than fluorescence decay. Depolarization also occurs much faster than the calculated rotational correlation time of a 10 nm diameter NP in water. Although the emission is polarized, the direction of the polarized emission is independent of the excitation polarization and different for each NP.

energy is quickly transferred to the lowest-energy point on the chain. The chromophore that ultimately emits a photon may or may not have its dipole moment aligned with the absorption dipole. This means that for individual fluorescent NPs, the absorption and emission by PFBT can give information on changes in the NP orientation. However, because of energy transfer, the excitation and emission polarizations may be randomly oriented with respect to each other. Figure 3B is an overlay of the time-resolved anisotropy decay and the fluorescence lifetime decay of polymer NPs in bulk aqueous solution. The high initial anisotropy of 0.36 may be due to emission from the initially excited chromophore, which was aligned with the polarized light and would be expected to be highly anisotropic. The subsequent decrease in bulk anisotropy would be caused by EET to a chromophore having a different emission dipole moment with little relation to the excitation polarization. Instead of decreasing to a perfectly isotropic value of 0, the fluorescence anisotropy decays to a final value of ~ 0.1 . There are several possible explanations for this residual anisotropy: (1) the fluorescent polymer may maintain some preferential orientation within the polymer NP; (2) chemical defects in the polymer chain may prevent transfer of a portion of the energy; or (3) a percentage of the light may be absorbed by the polymer's local energy minima, so a small additional amount energy transfer occurs. Integration under the anisotropic decay curve revealed that 94% of the photons were emitted after the anisotropic decay lifetime (τ_d); presumably, a large majority of these were emitted after EET. From the R_0 of 12.1 nm and the Perrin equation, we estimated the rotational correlation time (τ_r) of the polymer NPs to be 200 ns. The value of τ_d for the polymer NPs in bulk aqueous solution was 170 ps, which is 3 orders of magnitude shorter than τ_r and consistent with the time scale of EET along the polymer backbone.

Semiconducting polymer NPs as probes of microtubule orientation. The small size, optical stability, chemical flexibility, and polarization sensitivity of the polymer NPs makes them good candidates for use as probes to detect orientation changes in proteins. Eukaryotic microtubules inside cells usually contain 13 protofilaments (PFs) composed of repeating units of α and β tubulin; microtubules polymerized in vitro have been shown to consist of varying numbers of PFs. Variation away from 13 PFs per microtubule can create a periodic twist in the cylinder of the microtubule.^{23–25} The motor protein kinesin precesses along the PF axis in the microtubule, following any potential periodic twist in the microtubule axis. In a microtubule gliding assay, we passively adsorbed kinesin onto a glass surface to drive polymer-NP-labeled microtubules through a channel. As the microtubules were directed by kinesin, the periodicity of the microtubule twist could be visualized using fluorescence microscopy (Figure 4A).

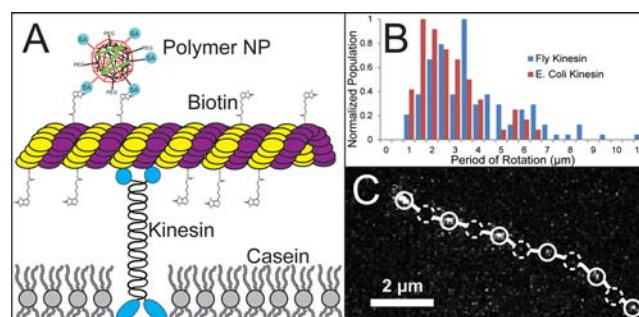


Figure 4. (A) Schematic illustration of a gliding microtubule moved by kinesin bound to a glass substrate. Polymer NPs are linked to biotinylated tubulin within the microtubule. (B) Periods of rotation measured for microtubules transported by two different forms of kinesin: 62 microtubules measured using *E. coli* kinesin and 131 measured using *Drosophila* kinesin, along with 69 and 171 nonrotating microtubules, respectively. (C) Track of a single microtubule with a single bound polymer NP. Unbroken and broken circles show local intensity maxima and minima, respectively, in one of the observed channels. The optical setup used to capture the image track is described in ref 19.

The heavy chain of kinesin is ~ 70 nm long, and the gliding assay was not inhibited by the presence of the 12 nm diameter polymer NPs. The periodicity of the microtubule twists was measured in this gliding assay using *Drosophila* kinesin and *Escherichia coli* kinesin, which have precession rates of 0.8 and 1.2 $\mu\text{m/s}$, respectively. We measured the precession rates of polymer-NP-labeled microtubules and microtubules containing fluorescent tubulin protein and found them to be the same. The polymer NPs did not appear to inhibit kinesin function. The measured microtubule twist length distributions for the slower *Drosophila* and faster *E. coli* kinesins remained consistent (Figure 4B). The twists were determined by the distance between local maxima in the polymer NP emission intensity and were not counted unless at least two consecutive periods of the same length between three local maxima were recorded. Also, the local intensity maxima and minima had to vary by at least 50%, representing a change in NP absorption/emission dipole orientation of ~ 0.75 radians over the course of the rotation. Figure 4C is a trace of a microtubule labeled with a single polymer NP, showing alternating bright and dark spots as the microtubule rotated. The observed numbers of rotating microtubules bound to the *Drosophila* and *E. coli* kinesins were 131 and 62, respectively. Along with polymer NPs that

periodically showed bright and dark emission, significant numbers of NPs showed continuous emission while bound to precessing microtubules. This could be due to the observation of microtubules made of 13 PFs, which do not have a twist, or alignment of the absorption/emission dipole of the NP with the microtubule. The latter case was considered unlikely, as often a single microtubule was labeled with several polymer NPs, and each such microtubule exhibited either periodic or constant emission from all of the bound NPs. We observed 171 nonrotating microtubules bound to the *Drosophila* kinesin and 69 nonrotating microtubules bound to *E. coli* kinesin.

The microtubules were polymerized with 10% biotinylated tubulin, which allowed strong binding between the SA-functionalized polymer NPs and the microtubules. Because of the high density of biotinylated tubulin and the size of the polymer NPs and tubulin units, it was likely that each polymer NP was bound to the microtubule by more than one biotin–SA linkage. There were virtually no fast, sporadic intensity fluctuations that would be evidence for single biotin–SA linkages or the “propeller effect” of polymer NPs with flexible attachments to microtubules.

In summary, we made small semiconducting polymer NPs with a low mass ratio of fluorescent polymer that have a strong sensitivity to polarization. The chromophore absorbs light and transfers energy to the energy minimum of the immobilized chain segment, which is responsible for the high degree of emission polarization. The fluorescent polymers were relatively short chains containing 20 monomers on average and made up a small mass percentage of the polymer NPs, so the remaining polymer shell prevented aggregation-induced quenching or collisional quenching by the solvent. By exciting the NPs with polarized light, we were able to measure the period of microtubule rotation. We anticipate the bright and polarization-sensitive probe described here will provide a useful tool for studying the rotational motions of biomolecules.

■ ASSOCIATED CONTENT

🔗 Supporting Information

Materials and methods and additional data. This material is available free of charge via the Internet at <http://pubs.acs.org>.

■ AUTHOR INFORMATION

Corresponding Author

chiu@chem.washington.edu

Notes

The authors declare no competing financial interest.

■ ACKNOWLEDGMENTS

We thank Dr. Mike Wagenbach and the Wordeman lab for providing kinesin, Dr. Lehui Xiao for preliminary work with P70-doped polymer NPs, and Bryant Fujimoto and Jiangbo Yu for input into the manuscript. This work was supported NIH (NS062725).

■ REFERENCES

- (1) Wu, C.; Chiu, D. T. *Angew. Chem., Int. Ed.* **2013**, *52*, 3086.
- (2) Wu, C.; Schneider, T.; Zeigler, M.; Yu, J.; Schiro, P. G.; Burnham, D. R.; McNeill, J.; Chiu, D. T. *J. Am. Chem. Soc.* **2010**, *132*, 15410.
- (3) Yu, J.; Wu, C.; Sahu, S. P.; Fernando, L. P.; Szymanski, C.; McNeill, J. *J. Am. Chem. Soc.* **2009**, *131*, 18410.
- (4) Hashim, Z.; Howes, P.; Green, M. *J. Mater. Chem.* **2011**, *21*, 1797.
- (5) Zhang, X.; Yu, J.; Wu, C.; Jin, Y.; Rong, Y.; Ye, F.; Chiu, D. T. *ACS Nano* **2012**, *6*, 5429.

(6) Rong, Y.; Wu, C.; Yu, J.; Zhang, X.; Ye, F.; Zeigler, M.; Gallina, M. E.; Wu, I.-C.; Zhang, Y.; Chan, Y.-H.; Sun, W.; Uvdal, K.; Chiu, D. T. *ACS Nano* **2013**, *7*, 376.

(7) Jin, Y.; Ye, F.; Zeigler, M.; Wu, C.; Chiu, D. T. *ACS Nano* **2011**, *5*, 1468.

(8) Wu, C.; Jin, Y.; Schneider, T.; Burnham, D. R.; Smith, P. B.; Chiu, D. T. *Angew. Chem., Int. Ed.* **2010**, *49*, 9436.

(9) Wu, C.; Hansen, S. J.; Hou, Q.; Yu, J.; Zeigler, M.; Jin, Y.; Burnham, D. R.; McNeill, J. D.; Olson, J. M.; Chiu, D. T. *Angew. Chem., Int. Ed.* **2011**, *50*, 3430.

(10) Petkau, K.; Kaeser, A.; Fischer, I.; Brunsveld, L.; Schenning, A. P. H. J. *J. Am. Chem. Soc.* **2011**, *133*, 17063.

(11) Chan, Y.-H.; Ye, F.; Gallina, M. E.; Zhang, X.; Jin, Y.; Wu, I.-C.; Chiu, D. T. *J. Am. Chem. Soc.* **2012**, *134*, 7309.

(12) Medina, C.; Santos-Martinez, M. J.; Radomski, A.; Corrigan, O. I.; Radomski, M. W. *Br. J. Pharmacol.* **2007**, *150*, 552.

(13) Zhou, Q.; Swager, T. M. *J. Am. Chem. Soc.* **1995**, *117*, 12593.

(14) Klärner, G.; Lee, J.-I.; Davey, M. H.; Miller, R. D. *Adv. Mater.* **1999**, *11*, 115.

(15) Nguyen, T.-Q.; Doan, V.; Schwartz, B. J. *J. Chem. Phys.* **1999**, *110*, 4068.

(16) Jakubiak, R.; Collison, C. J.; Wan, W. C.; Rothberg, L. J. *J. Phys. Chem. A* **1999**, *103*, 2394.

(17) Yu, J.; Hu, D.; Barbara, P. F. *Science* **2000**, *289*, 1327.

(18) Lakowicz, J. R. *Principles of Fluorescence Spectroscopy*, 3rd ed.; Springer: New York, 2006.

(19) Zeigler, M. B.; Allen, P. B.; Chiu, D. T. *Biophys. J.* **2011**, *100*, 2846.

(20) Lee, J.-I.; Zyung, T.; Miller, R. D.; Kim, Y. H.; Jeoung, S. C.; Kim, D. *J. Mater. Chem.* **2000**, *10*, 1547.

(21) Huser, T.; Yan, M.; Rothberg, L. J. *Proc. Natl. Acad. Sci. U.S.A.* **2000**, *97*, 11187.

(22) Schwartz, B. J.; Nguyen, T.-Q.; Wu, J.; Tolbert, S. H. *Synth. Met.* **2001**, *116*, 35.

(23) Chrétien, D.; Wade, R. R. *Biol. Cell* **1991**, *71*, 161.

(24) Sanghamitra, R.; Meyerhöfer, E.; Milligan, R. A.; Howard, J. *J. Cell Biol.* **1993**, *121*, 1083.

(25) Wang, G.; Sun, W.; Luo, Y.; Fang, N. *J. Am. Chem. Soc.* **2010**, *132*, 16417.